

CHAPTER 172

ENERGY DISSIPATION AND WAVE FORCE AT SLOTTED WALL

Saburo URASHIMA¹, Koichi ISHIZUKA² and Hideo KONDO³

Abstract

The hydrodynamic coefficients are computed based on the measured total force on the single slotted wall in the wave field, or on the measured head loss in the uniform flow channel. The reflection, transmission and force coefficients on the single slotted wall are computed based on the mean values of the hydrodynamic coefficients. The correlations between these calculated values and measured values are found to be good. A design procedure of the single slotted wall is given the paper.

1 INTRODUCTION

Many studies on wave energy dissipating structures using a pervious wall have been carried out mainly for caisson-type breakwaters, which have a chamber between the pervious front wall and the solid backwall. Although the hydrodynamic characteristics of the single pervious wall are not well-known, it is not so well-known that it can serve as a breakwater itself. The objective of this paper is to establish the optimum form of the vertical parallel piled slits by obtaining the coefficients of reflection, transmission and wave force which are estimated by the drag and mass coefficients.

The hydrodynamic coefficients are computed by measuring the total force on the slotted wall and then employing Morison's equation and the small amplitude wave theory in the wave field, or by measuring the head loss in the uniform flow channel. The reflection and transmission coefficients are determined by making use of the analytical approach to the small amplitude shallow water wave deformation at the pervious wall as explained by the last author in 1979.¹⁾

2 EXPERIMENTAL SETUP

The experiments were conducted in a wave flume 0.8 meter deep, 0.4 meter wide and 19.7 meter long. For each test a slotted wall orientation was kept perpendicular to the incident wave direction. The range of wave parameters were as follows:

Wave steepness H_I/L : 0.002 to 0.056

Relative depth h/L : 0.100 to 0.281

The water depth was kept constant at 0.5 meter throughout the experiment. The test apparatus which was used for measurement of wave force is illustrated schematically in Fig. 1. The slotted wall which was tested for measurement of wave force consisted of an acrylic wall, 0.4 meter in width and 0.6 meter long, supported on two frames which were

1 Assistant Professor of Civil Engineering, Tomakomai College of Technology, 443 Nishikioka, Tomakomai, 059-12 JAPAN

2 Professor of Civil Engineering, ditto

3 Professor of Civil Engineering, Muroran Institute of Technology, 27-1 Mizumoto-Cho, Muroran, 050 JAPAN

suspended from the wave flume. These frames were made of steel, 25 by 16 millimeter in section. The wave force was transmitted to the strain-gauges on these frames. Two-dimensional flume tests were made. The reflection coefficients have been computed using Heal's formula.

In addition, the head loss was measured in the uniform flow channel. 21 types of the models with various void ratios and wall thicknesses were tested, as shown in table 1.

3 PROCEDURES EMPLOYED

The ratio of reflected wave amplitude a_r and the incident wave amplitude a_i can be estimated analytically as

$$\frac{a_r}{a_i} = \frac{A_{0,1}}{2 + A_{0,1}} = \frac{\frac{\sigma}{kh} \left[\frac{C_l}{2g} |u_{1,1}| + i \frac{\sigma \mathcal{L}}{g} \right]}{2 + \frac{\sigma}{kh} \left[\frac{C_l}{2g} |u_{1,1}| + i \frac{\sigma \mathcal{L}}{g} \right]}$$

(1)

Also the ratio of transmitted wave amplitude a_t to incident wave amplitude is given by

$$\frac{a_t}{a_i} = \frac{2}{2 + A_{0,1}} = \frac{2}{2 + \frac{\sigma}{kh} \left[\frac{C_l}{2g} |u_{1,1}| + i \frac{\sigma \mathcal{L}}{g} \right]}$$

(2)

where σ is $2\pi/T$ and k is $2\pi/L$. The absolute value of the water particle velocity $|u_{1,1}|$ is approximated by

$$|u_{1,1}| = \frac{8}{3\pi} U_{1,1} \tag{3}$$

where $U_{1,1}$ is the amplitude of horizontal water particle velocity, C_l is the head loss coefficient and \mathcal{L} is the apparent orifice length.

The forces are divided into two parts, one due to the drag in the case of constant flow, and the other due to acceleration or deceleration of the fluid. The horizontal total force on a slotted wall is given by

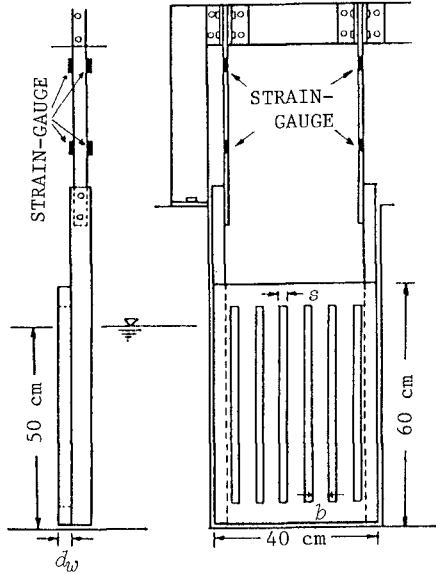


FIG. 1 TEST SETUP FOR THE SLOTTED WALL

Table 1 Geometry of Slotted Walls

| Standard Slotted Wall | | | | |
|------------------------|----------|----------|------------|---------|
| λ (%) | b (mm) | s (mm) | d_w (mm) | d_w/s |
| 25 | 50 | 17 | 15 | 0.90 |
| | | | 30 | 1.80 |
| | | | 45 | 2.70 |
| 35 | 43 | 23 | 15 | 0.64 |
| | | | 30 | 1.29 |
| | | | 45 | 1.93 |
| 50 | 33 | 33 | 15 | 0.45 |
| | | | 30 | 0.90 |
| | | | 45 | 1.35 |
| Array of Square Column | | | | |
| λ (%) | b (mm) | s (mm) | d_w (mm) | d_w/s |
| 20 | 40 | 10 | 15 | 1.50 |
| | | | 30 | 3.00 |
| | | | 45 | 4.50 |
| 30 | | 17 | 15 | 0.88 |
| | | | 30 | 1.75 |
| | | | 45 | 2.63 |
| 40 | | 27 | 15 | 0.56 |
| | | | 30 | 1.12 |
| | | | 45 | 1.69 |
| 50 | 40 | 40 | 15 | 0.38 |
| | | | 30 | 0.75 |
| | | | 45 | 1.13 |

$$F_T(t) = F_D(t) + F_I(t) = C_D \cdot f_D(t) + C_M \cdot f_I(t) \quad (4)$$

in which

$$f_D(t) = \int_{-h}^{\eta} \rho \frac{u|u|}{2} dA \quad (5)$$

and

$$f_I(t) = \int_{-h}^{\eta} \rho \dot{u} dV \quad (6)$$

and $F_T(t)$ is the horizontal total force, $F_D(t)$ is the horizontal drag force, $F_I(t)$ is the horizontal inertia force, ρ is the mass density of water, η is the water surface elevation, dA and dV refer to the small projected area and volume, u and \dot{u} are particle velocity and acceleration and C_D , C_M are the drag and mass coefficients, respectively.

The force coefficient f is defined as

$$f = \frac{F_{max}}{\rho g (1-\lambda) B h d_w} \quad (7)$$

where F_{max} is maximum total force, g is acceleration of gravity, B is wall width and h is water depth.

The relationship between the head loss coefficient C_i and the drag coefficient C_D is given by

$$C_i = (1-\lambda) \cdot C_D \quad (8)$$

and the relationship between the apparent orifice length \mathcal{L} and the mass coefficient C_M is given by

$$\mathcal{L} = \left[1 + \frac{(1-\lambda) \cdot C_M}{\lambda} \right] \cdot d_w \quad (9)$$

where λ is the void ratio, d_w is the wall thickness.

4 RESULTS

4.1 Hydrodynamic Coefficient

Fig. 2 presents the head loss coefficients from the wave and from the uniform flow tests. The head loss coefficients from wave test and those from uniform flow test formed smooth continue curve. Evidently, there is a remarkable correlation between the head loss coefficients and Reynolds number. The head loss coefficient is estimated with the Reynolds number Re , as follows.

$$C_i = \frac{A_1}{Re} + B_1 \quad (10)$$

where A_1 and B_1 are constants determined by the experiment. Reynolds number Re is defined by the following equation.

$$Re = \frac{u_{r.m.s} \cdot S}{\nu} \quad (11)$$

where

$$u_{r.m.s} = \frac{1}{T} \sum_{i=1}^N \sqrt{\frac{\int_{-h}^{\eta} u^2 dy}{h + \eta}} \Delta t \quad (12)$$

and $u_{r.m.s}$ is the root-mean-square velocity. Here $u_{r.m.s}$ is adapted as the presentative velocity.

Fig. 3 shows the head loss coefficient for a standard slotted wall, and Fig. 4 shows one for an array of square columns in uniform flow. In turbulent flow, the head loss coefficient is constant. The head

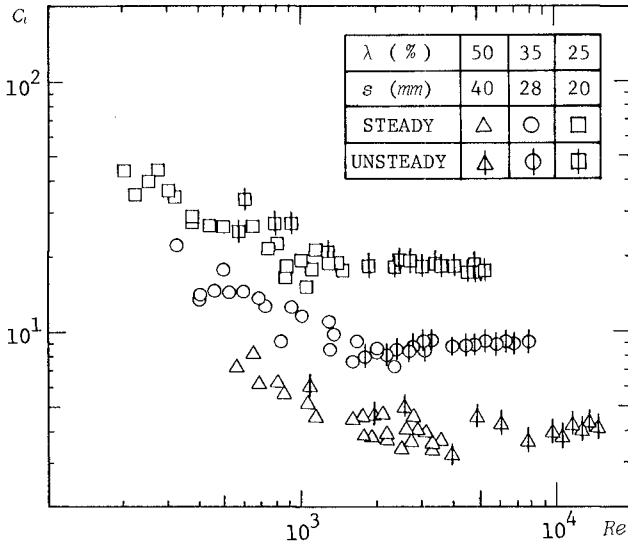


FIG. 2 HEAD LOSS COEFFICIENT VERSUS REYNOLDS NUMBER
($d_w = 30$ mm)

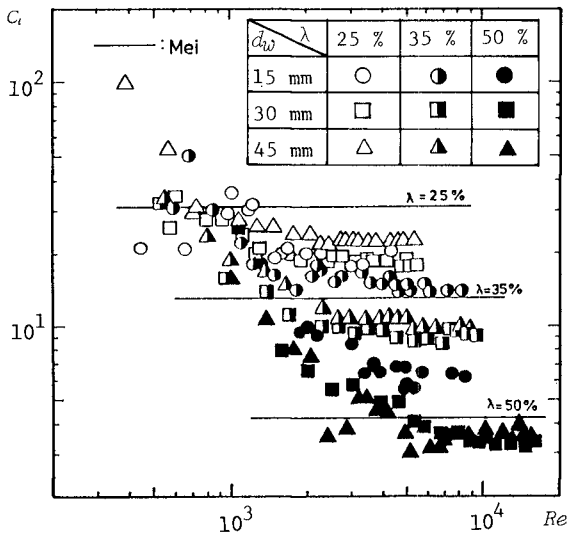


FIG. 3 HEAD LOSS COEFFICIENT VERSUS REYNOLDS NUMBER

loss coefficient is considered to be a function of the void ratio, wall thickness and slit width. The head loss coefficient is approximated by

$$C_l = B_1 = \frac{0.52}{\lambda^{3.0} (d_w/s)^{0.46}} \quad (13)$$

Fig. 5 shows the apparent orifice length versus Keulegan-Carpenter number KC . Evidently, there is a remarkable correlation between the apparent orifice length, wave length and Keulegan-Carpenter number. The apparent orifice length is given as a function of the wave length and the Keulegan-Carpenter number as follows.

$$\frac{\bar{x}}{L} = \frac{A_2}{KC} + B_2 \quad (14)$$

where A_2 and B_2 are constants determined by the experiment. Keulegan-Carpenter number is defined by the following equation.

$$KC = \frac{u_{r.m.s.} \cdot T}{d_w} \quad (15)$$

where T is the wave period and d_w is the wall thickness. The constant B_2 is given as a function of the wall thickness as follows.

$$\frac{\bar{x}}{L} = B_2 = 0.00567 \cdot d_w + 0.0033 \quad (16)$$

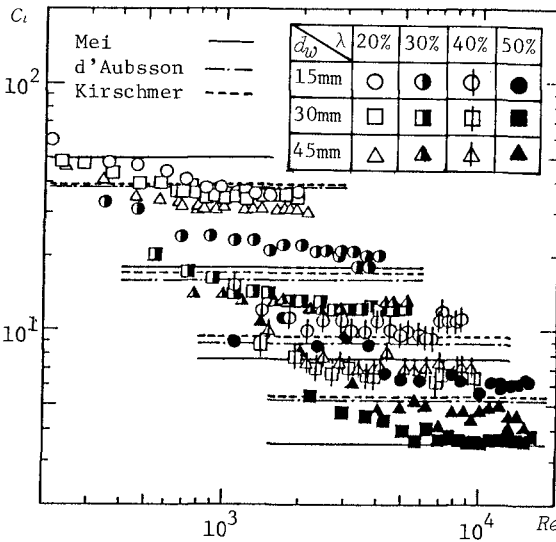


FIG. 4 HEAD LOSS COEFFICIENT VERSUS REYNOLDS NUMBER

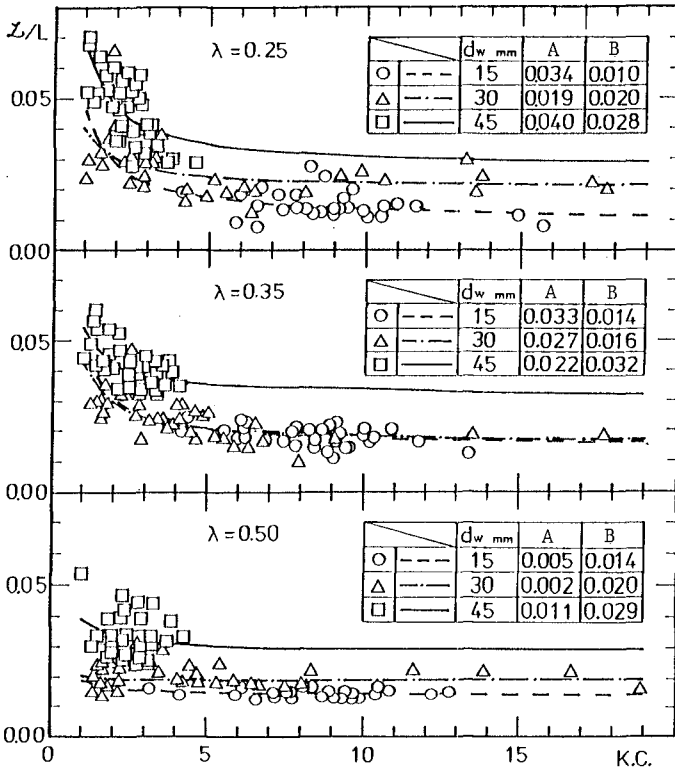


FIG. 5 RATIO OF APPARENT ORIFICE LENGTH TO WAVE LENGTH VERSUS KEULEGAN-CARPENTER NUMBER

4.2 The Reflection Coefficient and Transmission Coefficient

Fig. 6 shows the reflection coefficient K_R and the transmission coefficient K_I versus the wave steepness H/L for the various values of relative water depth h/L . The theoretical results of Kondo(1979) using an experimental coefficient are superimposed for comparison with the results of the experiment. The agreement between the theoretical and actual results of the experiment is found to be relatively good. In this figure, as the incident wave height increases in the range of smaller height, the reflection coefficient decreases to a certain minimum value, and then increases as the wave height further increases, meanwhile, the transmission coefficient increases to a certain maximum value, and decreases afterwards. It is seen that the wave steepness has an important influence on the reflection and transmission coefficients.

Fig. 7 shows the dependence of reflection and transmission coeffi-

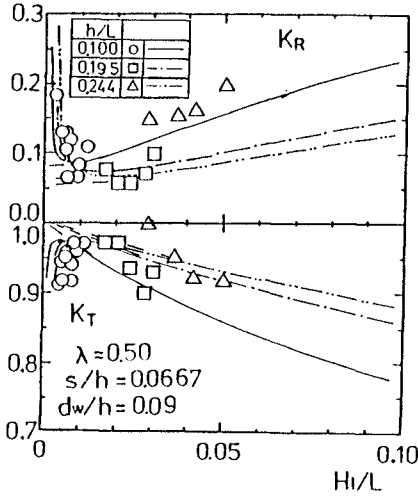


FIG. 6 REFLECTION AND TRANSMISSION COEFFICIENT VERSUS WAVE STEEPNESS

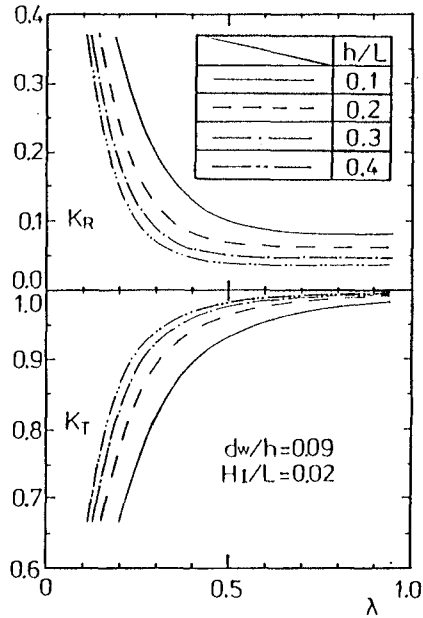


FIG. 7 REFLECTION AND TRANSMISSION COEFFICIENT VERSUS VOID RATIO

coefficients on the void ratio λ for the various values of relative depth. In this figure, the reflection coefficient decreases rapidly as void ratio increases and gradually decreases to a certain value, while the transmission coefficient increases in the similar manner. It is seen that the void ratio has a great effect on the reflection and transmission coefficients. With wider spacing between the square piles greater energy will be transmitted than reflected or lost and hence the transmission coefficient increases with the void ratio. As the slit size becomes very large, however the effectiveness of the slotted wall as an energy dissipator decreases. The reflection coefficient decreases with increasing slit size as was expected. This can be attributed to the reduction in the net projected area of the slotted wall normal to the direction of wave advance giving rise to greater transmitted energy

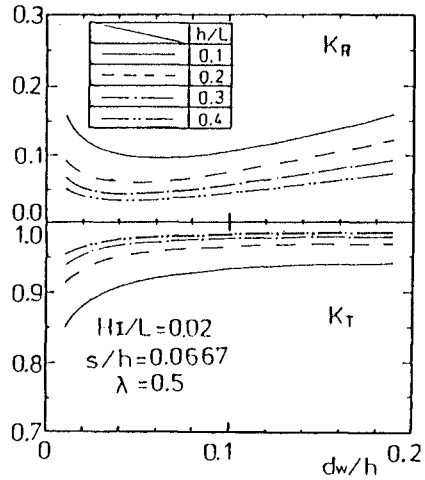


FIG. 8 REFLECTION AND TRANSMISSION COEFFICIENT VERSUS d_w/h

and lesser reflected energy.

Fig. 8 shows the variation of reflection and transmission coefficients with the ratio of wall thickness to water depth d_w/h for the various values of relative depth. In this figure, the reflection and transmission coefficients are not sensitive to the wall thickness. The reflection coefficient decreases as relative water depth increases, and the transmission coefficient increases slightly as relative water depth increases.

4.3 The Force Coefficient

Fig. 9 shows the force coefficient f of Eq.7 versus the wave steepness for the various values of relative depth. The force coefficient increases with wave steepness as expected. The theoretical values which are indicated by the lines on the chart show good agreement with the experimental results within the range of lower values of wave steepness.

Fig. 10 shows the force coefficient versus the void ratio λ for the various values of relative depth. In this figure, the force coefficient decreases at first, then keeps almost constant and increases afterwards, as the void ratio increases. It decreases as the wall thickness increases, and as relative water depth increases.

5 CONCLUSIONS

There is a remarkable correlation between the head loss coefficient and Reynolds number. There is a remarkable correlation between the apparent orifice length, Keulegan-Carpenter number and wave length.

We suggested that the head loss coefficient is given as a function of the void ratio, wall thickness and slit width. We suggested that the apparent orifice length is given as a function of wall thickness.

The theoretical results using these experimental coefficients show relatively good agreement with the results of the experiment.

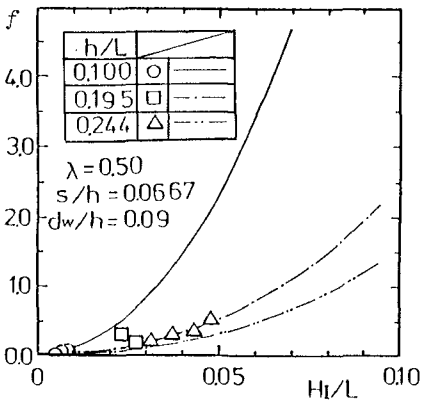


FIG. 9 FORCE COEFFICIENT VERSUS WAVE STEEPNESS

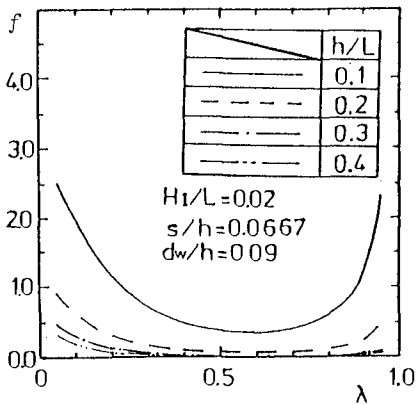


FIG. 10 FORCE COEFFICIENT VERSUS VOID RATIO

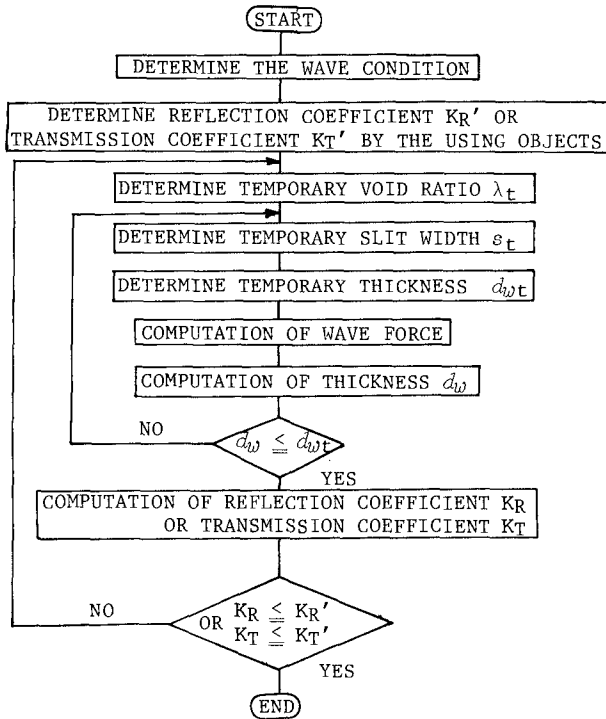


FIG. 11 DESIGN PROCESS OF THE SINGLE PERVIOUS WALL

The optimum void ratio of the slotted wall lies around 0.2 to 0.4 and corresponds to the required conditions of the wall, since the rates of change of the force, reflection and transmission coefficients are large in that range. It can therefore be concluded that using the design process for a single pervious wall to serve as a breakwater, as indicated in Fig. 11 will be effective. The initial value of the void ratio, slit width and thickness may be obtained from fig. 6 to 8. However, the actual wall thickness must take into account the level of wave force. In the case of a constant wall thickness, the reflection coefficient can be decreased by increasing the slit width.

REFERENCES

- 1) Kondo, H. :Analysis of breakwaters having two porous walls, Coastal Structures '79, ASCE, vol. II, 962-977, 1979.